THE BELL SYSTEM TECHNICAL JOURNAL
Vol. 59, No. 6, July–August 1980
Printed in U.S.A.

Microwave Depolarization of an Earth-Space Path*

By T. S. CHU

(Manuscript received January 17, 1980)

The nonspherical shapes of both rain and ice particles contribute to microwave depolarization on an earth-space path. A two-tier Gaussian model for rain, which assumes Gaussian distributions both for instantaneous canting angle and time-varying mean canting angle, together with gross features of ice particles, provides a theoretical framework to organize the experimental data and to yield functional dependence of cross polarization on freqency, polarization, and elevation angle. In spite of the lack of physical data on ice clouds, we have obtained agreement between measured depolarization data and theoretical results that are essentially independent of details of ice clouds. In particular, we have found a linear relation between cross-polarization amplitude and frequency throughout the centimeter wavelengths for a given earth-space path. The dependence of depolarization on orientation of an arbitrary linear polarization can be described by a simple, nearly sinusoidal expression that is relatively insensitive to the mean canting angle except within about ten degrees of the local "vertical" or horizontal direction. We show measured depolarization data for paths of various elevation angles to be consistent with each other using an empirical effective path length and the approximate $\cos^2 \theta_{el}$ factor for the differential attenuation and differential phase shift. Procedures of estimating cross polarizations for satellite communication systems and typical numerical results are summarized.

I. INTRODUCTION

Investigation of depolarization of an earth-space path is motivated by the planning of frequency reuse in dual-polarization satellite communication systems. Since an earth-space path is usually free of multipath fading, microwave depolarization will be contributed essen-

* Part of this paper was presented at the 1979 USNC/URSI spring meeting, Seattle Washington.

tially by rain and ice particles. The lack of physical data of ice clouds prevents precise predictions. However, a theoretical framework to organize the experimental data can be established upon the gross features of the ice particles and the extrapolation of terrestrial rain models.[1-3] We look for functional dependence of cross polarization on frequency, polarization, elevation angle, and rain rate in order for existing experimental data[4-11] to serve system planners. For example, systematic extrapolation of 19/28 GHz COMSTAR beacon measurements to 4/6 GHz is needed for the current design of the second generation of AT&T satellites.

It is now well known that rain-induced differential attenuation and differential phase shift cause microwave depolarization. In this paper, the differential attenuation and differential phase shift on earth-space paths between polarizations perpendicular and parallel to the plane of incidence (i.e., that plane which contains the directions of propagation and raindrop axis of symmetry) will be approximated by

$$\alpha_2 - \alpha_1 = (\alpha_2 - \alpha_1)_{\theta_{el}=0}\cos^2\theta_{el}$$
$$\beta_2 - \beta_1 = (\beta_2 - \beta_1)_{\theta_{el}=0}\cos^2\theta_{el}, \tag{1}$$

where the terrestrial cases of $\theta_{el=0}$ are simply those between polarizations perpendicular and parallel to the axis of symmetry of oblate raindrops. This approximation, which was checked by previous numerical calculations when the raindrop axis of symmetry is vertical,[1] is very useful, since extensive data are available for the terrestrial case.[2]

The satellite elevation angle affects not only the differential attenuation and differential phase shift of raindrops but also the effective path length, which is a very important parameter for depolarization statistics. We make use of an empirical formula for effective path length, which was previously developed for estimating rain attenuation distribution:[12]

$$L = \frac{h/\sin\theta_{el}}{1 + [(h/\sin\theta_{el})/\bar{L}]}, \tag{2a}$$

where

$$\bar{L} = \frac{2636}{R - 6.2}\ \text{km}, \tag{2b}$$

R is the five-minute point rain rate in mm/hr, θ_{el} is the satellite elevation angle, and the rain height h is assumed to be 4 km.

For an area-coverage or a scanning spot-beam satellite, the antenna polarization seen from earth stations is often neither "vertical" nor horizontal. The following model appears convenient for the treatment

of an arbitrary linear polarization: Let the microwave propagation through rainstorms be simulated by a random uniaxial, anisotropic medium with the anisotropies given by the aforesaid differential attenuation and differential phase shift. The instantaneous orientation of its axis of anisotropy, which is the projection of the raindrop axis of symmetry onto the plane perpendicular to the direction of propagation,* will be Gaussian-distributed over the path with time-varying mean θ_m and a standard deviation of σ_θ. Over the long term, θ_m is also assumed to be Gaussian-distributed over various rainstorms with zero mean and a standard deviation of σ_m. This two-tier Gaussian distribution is an extension of the single Gaussian distribution[3,14] in order to provide nonzero rain-induced cross polarization (averaged over various rainstorms) for all linear polarizations.

Ice particles also contribute to depolarization. Very little is known about ice particles except that they are small compared with centimeter wavelength and have an essentially lossless dielectric constant of 3. However, this observation together with the rain-model calculations will lead us to an important prediction of a simple linear relation between cross-polarization amplitude and frequency.

II. CALCULATIONS

Let a pair of orthogonal linear polarizations be designated quasi-vertical V and quasi-horizontal H according to their proximities to the local vertical and horizontal directions, respectively. The quasi-vertical polarization is oriented at an angle $\tau \leq 45°$ from the vertical plane of incidence which contains the directions of propagation and local gravity. For an anisotropic medium with the axis of anisotropy at an angle θ from this vertical plane of incidence, the polarization transformations can be easily obtained by the multiplication of the following matrices:

$$\begin{pmatrix} H_r \\ V_r \end{pmatrix} = \begin{pmatrix} \cos(\theta-\tau) & -\sin(\theta-\tau) \\ \sin(\theta-\tau) & \cos(\theta-\tau) \end{pmatrix} \begin{pmatrix} T_2 & 0 \\ 0 & T_1 \end{pmatrix} \cdot \begin{pmatrix} \cos(\theta-\tau) & \sin(\theta-\tau) \\ -\sin(\theta-\tau) & \cos(\theta-\tau) \end{pmatrix} \begin{pmatrix} H_t \\ V_t \end{pmatrix}, \quad (3)$$

where T_2 and T_1 are transmission coefficients over a path length L for polarizations perpendicular and parallel, respectively, to the axis of anisotropy,

$$T_2 = \exp[-(\alpha_2 - j\beta_2)L] \quad (4)$$

$$T_1 \exp[-(\alpha_1 - j\beta_1)L]. \quad (5)$$

* The random component parallel to the vertical plane of incidence is expected to contribute a variation in cross-polarization signal level of less than 1 dB (Ref. 13).

Then the relationship between transmitted and received polarizations will be

$$\begin{pmatrix} H_r \\ V_r \end{pmatrix} = \begin{pmatrix} a_{hh} & a_{hv} \\ a_{vh} & a_{vv} \end{pmatrix} \begin{pmatrix} H_t \\ V_t \end{pmatrix}, \tag{6}$$

where

$$a_{hh} = \frac{T_2 + T_1}{2} + \frac{T_2 - T_1}{2} \cos 2(\theta - \tau) \tag{7}$$

$$a_{vv} = \frac{T_2 + T_1}{2} - \frac{T_2 - T_1}{2} \cos 2(\theta - \tau) \tag{8}$$

$$a_{hv} = a_{vh} = \frac{T_2 - T_1}{2} \sin 2(\theta - \tau). \tag{9}$$

If, at a given instant, θ is a Gaussian-distributed random variable with a standard deviation of σ_θ and a mean value of θ_m, the expected values of the above matrix elements are

$$\overline{a_{hh}} = \frac{T_2 + T_1}{2} + \frac{T_2 - T_1}{2} \cos 2(\theta_m - \tau) e^{-2\sigma_\theta^2} \tag{10}$$

$$\overline{a_{vv}} = \frac{T_2 + T_1}{2} - \frac{T_2 - T_1}{2} \cos 2(\theta_m - \tau) e^{-2\sigma_\theta^2} \tag{11}$$

$$\overline{a_{hv}} = \overline{a_{vh}} = \frac{T_2 - T_1}{2} \sin 2(\theta_m - \tau) e^{-2\sigma_\theta^2} \tag{12}$$

The corresponding power coefficients are

$$|\overline{a_{hh}}|^2 = \exp[-(\alpha_1 + \alpha_2)L][D + C \cos^2 2(\theta_m - \tau) e^{-4\sigma_\theta^2} - E \cos 2(\theta_m - \tau) e^{-2\sigma_\theta^2}] \tag{13}$$

$$|\overline{a_{vv}}|^2 = \exp[-(\alpha_1 + \alpha_2)L][D + C \cos^2 2(\theta_m - \tau) e^{-4\sigma_\theta^2} + E \cos 2(\theta_m - \tau) e^{-2\sigma_\theta^2}] \tag{14}$$

$$|\overline{a_{hv}}|^2 = |\overline{a_{vh}}|^2 = \exp[-(\alpha_1 + \alpha_2)L] C \sin^2 2(\theta_m - \tau) e^{-4\sigma_\theta^2}, \tag{15}$$

where

$$C = \sinh^2 \alpha L + \sin^2 \beta L \tag{16}$$

$$D = \cos^2 \beta L + \sinh^2 \alpha L \tag{17}$$

$$E = 2 \cosh \alpha L \sinh \alpha L \tag{18}$$

$$2\alpha = \Delta\alpha = (\alpha_2 - \alpha_1) \quad \text{and} \quad 2\beta = \Delta\beta = (\beta_2 - \beta_1). \tag{19}$$

Now if the time-varying mean canting angle θ_m is also Gaussian-distributed over various rainstorms with zero mean and a standard deviation of σ_m, then integrating over this distribution will yield the

long-term average expected attenuation and cross-coupling coefficients:

$$\left.\begin{matrix}\overline{|\overline{a_{hh}}|^2} \\ \overline{|\overline{a_{vv}}|^2}\end{matrix}\right\} = \exp[-(\alpha_1 + \alpha_2)L]$$

$$\cdot\left\{D + \frac{Ce^{-4\sigma_\theta^2}}{2}[1 + \cos 4\tau\, e^{-8\sigma_m^2}] \mp E \cos 2\tau\, e^{-2(\sigma_\theta^2 + \sigma_m^2)}\right\} \quad (20)$$

$$\overline{|\overline{a_{hv}}|^2} = \overline{|\overline{a_{vh}}|^2} = \exp[-(\alpha_1 + \alpha_2)L]\frac{Ce^{-4\sigma_\theta^2}}{2}[1 - \cos 4\tau\, e^{-8\sigma_m^2}]. \quad (21)$$

Dividing eq. (21) by eqs. (20) will give the cross polarization of linearly polarized waves:

$$\overline{XPL} = \frac{1}{2}\left(\frac{C}{D}e^{-4\sigma_\theta^2}\right)(1 - \cos 4\tau\, e^{-8\sigma_m^2})\delta, \quad (22)$$

where the quantity in the first parenthesis will be identified below in eq. (25) as rain-induced cross polarization of circularly polarized waves. The differential attenuation factor δ is the ratio between eqs. (25) and (20). When the differential attenuation is small, $|10 \log_{10}\delta|$ is approximately half of the differential attenuation ΔA between quasi-horizontal and quasi-vertical polarizations, i.e.,

$$|10\, log_{10}\delta| \approx \frac{\Delta A}{2} = 5 \log_{10}(\overline{|\overline{a_{vv}}|^2}/\overline{|\overline{a_{hh}}|^2}). \quad (22a)$$

Since σ_m is small compared with unity, the cross polarization of a linearly polarized wave with $\tau = 45°$ is almost the same as that of a circularly polarized wave.

Since a circularly polarized wave can be treated as two orthogonal linearly polarized components in phase quadrature, its polarization ratio can be obtained from the following transformation:

$$\begin{pmatrix} H \\ V \end{pmatrix} = \begin{pmatrix} a_{hh} & a_{hv} \\ a_{vh} & a_{vv} \end{pmatrix}\begin{pmatrix} 1 \\ j \end{pmatrix}. \quad (23)$$

The ratio of the undesired rain-induced circular polarization to the desired circular polarization is[15]

$$\left(1 + j\frac{V}{H}\right)\Big/\left(1 - j\frac{V}{H}\right).$$

From eq. (23), the cross polarization of circular polarization becomes

$$\overline{XPC} = (|a_{vh}/a_{hh}|^2_{(\theta-\tau)=45°})\,|\overline{e^{j2\theta}}|^2 = \frac{C}{D}e^{-4\sigma_\theta^2}. \quad (24)$$

σ_m is absent in eq. (24) because the cross polarization of circularly polarized waves is independent of the mean orientation of raindrops. The power attenuation coefficient of a circularly polarized wave is simply

$$A_c = D \exp[-(\alpha_1 + \alpha_2)L]. \tag{25}$$

Expanding eqs. (16) and (17) gives

$$\frac{C}{D} = (\alpha L)^2\left[1 - \frac{2(\alpha L)^2}{3} + \cdots\right] + (\beta L)^2\left[1 + \frac{2(\beta L)^2}{3} + \cdots\right]. \tag{26}$$

When αL (in nepers) and βL (in radians) are small, D is approximately unity and, using eq. (19),

$$\frac{C}{D} \approx \frac{1}{4}(\sqrt{(\Delta\alpha)^2 + (\Delta\beta)^2}L)^2 \tag{27}$$

which indicates the proportionality between rain-induced cross-polarization amplitude and differential propagation constant.

The effects of ice particles are not included in eqs. (22) and (24). A correction factor for ice-induced cross polarization will be determined by the comparison between numerical results and measured data.

III. NUMERICAL RESULTS AND DISCUSSIONS

3.1 Circular polarization

Now let us test the proposed model with the measured data of received signals from satellite beacons. We first make the comparison between calculated and measured results for depolarization of circularly polarized waves versus attenuation as shown in Figs. 1 through 3. Previous measurements of differential attenuation[1,16] and photographs of falling raindrops[17] suggest 30° as the probable value for σ_θ. The calculated curves are obtained from eqs. (24) and (25) for each of a sequence of rain rates. Measured data[4] in Fig. 1 are determined[5] from measured results of the complete transmission matrix of two orthogonal linear polarizations (21° and 69° from the vertical plane of incidence) of the COMSTAR beacon. Measured points in Fig. 2 were obtained by A. J. Rustako from the CTS 11.7-GHz circularly polarized beacon.[7] The measured curve in Fig. 3 represents rain depolarization measurement using INTELSTAT-IV at Yamaguchi, Japan.[8]

In each comparison at three separate frequencies and elevation angles, the measured data, all of which are median values, show a consistent discrepancy of about 2 dB above the calculated curves. The measured values are expected to be higher than those predicted for rain because of other depolarization effects such as those due to ice particles. The residual system cross polarizations in clear weather are

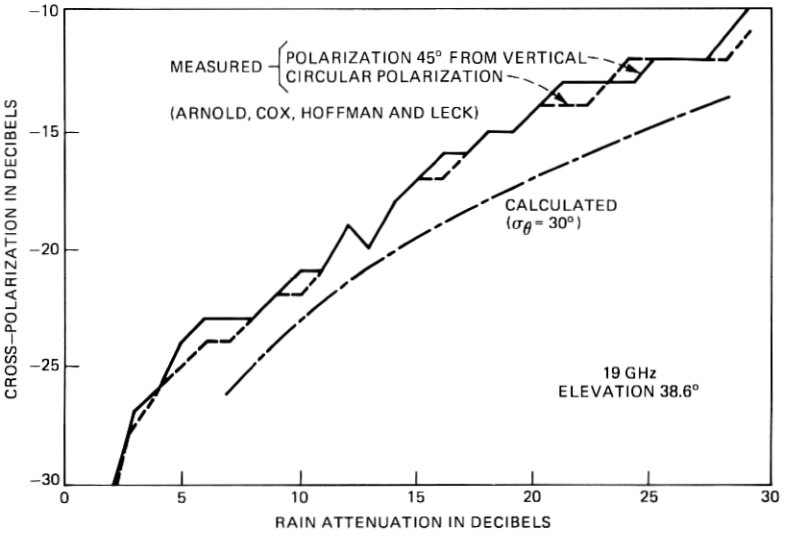

Fig. 1—Comparison between calculated rain-induced cross polarization and measured data from COMSTAR II. Higher measured values are expected due to ice particle contributions. The standard deviation of raindrop canting-angle distribution is σ_θ.

negligible in Fig. 1, -33 dB for Fig. 2, and −23.5 dB for Fig. 3. At the lower end of attenuation values, the depolarization effects of ice particles become predominant. Since the cross-polarization level remains low here, any uncertainty of its prediction is tolerable in system engineering. The larger discrepancy at the higher end of attenuation values may be attributed to either small sample size or shortcoming of the model. However, the consistent picture in the range of moderate cross polarization ($\lesssim -10$ dB) indicates reliable predictions of the model (including 2-dB correction for ice particles) in this most interesting range for system planning and suggests that the measured data are predictable from each other.

3.2 Frequency dependence

Equation (27) implies that the cross-polarization amplitude is approximately proportional to the differential propagation constant $\sqrt{(\Delta\alpha)^2 + (\Delta\beta)^2}$. In Fig. 2, we show that this approximation holds very well up to a cross-polarization level of about −10 dB, where the discrepancy is less than 0.5 dB. Using the previously calculated rain-induced differential attenuation and differential phase shift,[2] Fig. 4 presents the differential propagation constant for various rain rates from 4 through 30 GHz. It is seen that the differential propagation constant is proportional to frequency practically throughout the centimeter wavelength range. Only in the upper end of this frequency

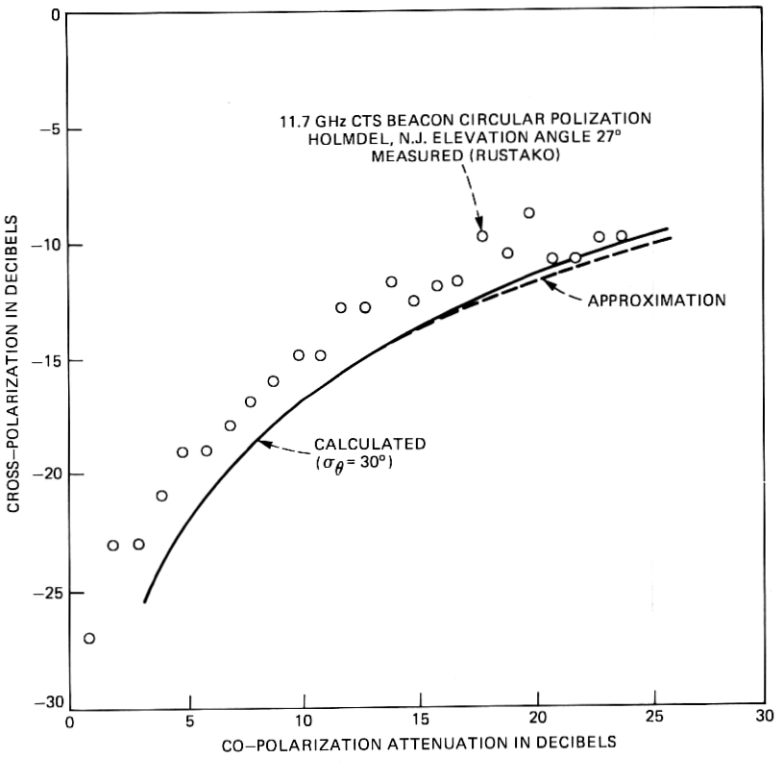

Fig. 2—Comparison between calculated rain-induced cross polarization and measured data from CTS beacon. The dotted curve is an approximation using eq. (27) for small differential attenuation and differential phase shift. Higher measured values are expected due to ice particle contributions.

range at very heavy rain rates does the deviation from linear dependence begin to appear. At lower microwave frequencies where the differential attenuation is negligible, the differential phase shift is proportional to the frequency.[2] As the frequency increases, the rise in differential attenuation just makes up for the slowdown of the increase in differential phase shift to maintain the linear dependence on frequency for a given amount of rain.

The other contributor to depolarization on an earth-space path is the effect of small lossless ice particles. They are expected to be free of differential attenuation, and their microwave differential phase shifts, which obey the Rayleigh approximation, are certainly also proportional to frequency. The above arguments lead us to an important conclusion for frequency extrapolation, that is, the simple linear relation between cross-polarization amplitude and frequency for a given earth-space path. A direct confirmation of this prediction is shown in Fig. 5, where the two solid curves are measured cross-

polarization statistics at 19 and 28.5 GHz[4] received from the COMSTAR beacon at 38.6° elevation angle with the transmitting polarization at 21° from the vertical plane of incidence. The three dotted curves are linear frequency extrapolations from the measured curve of 19 GHz. The measured statistics of 28.5 GHz show slightly smaller cross polarization than the prediction of linear frequency extrapolation just as expected from the differential propagation constant data for this frequency range in Fig. 4.

In the absence of measured depolarization statistics at lower frequencies for the same satellite elevation angle, let us test the frequency extrapolation by comparing measured cross polarization versus rain attenuation data from the 11.7-GHz CTS beacon at 27° elevation angle with results obtained by extrapolation from the 19-GHz COMSTAR beacon at 38.6° elevation angle. The dotted curve in Fig. 6 is predicted from the 19-GHz measurements using the procedure described in Section 4.2.2 and shows good agreement with the measured 11.7-GHz CTS data. One notes that this process of extrapolation is insensitive to the raindrop model, the assumed canting angle standard deviation, and the empirical expression for the effective path length.

3.3 Elevation angle dependence

It is also interesting to check the elevation angle dependence by comparing the depolarization data obtained from the same 11.7-GHz CTS beacon at different locations. The CTS depolarization data were also available at Austin, Texas with an elevation angle of 49.5°[9] and at

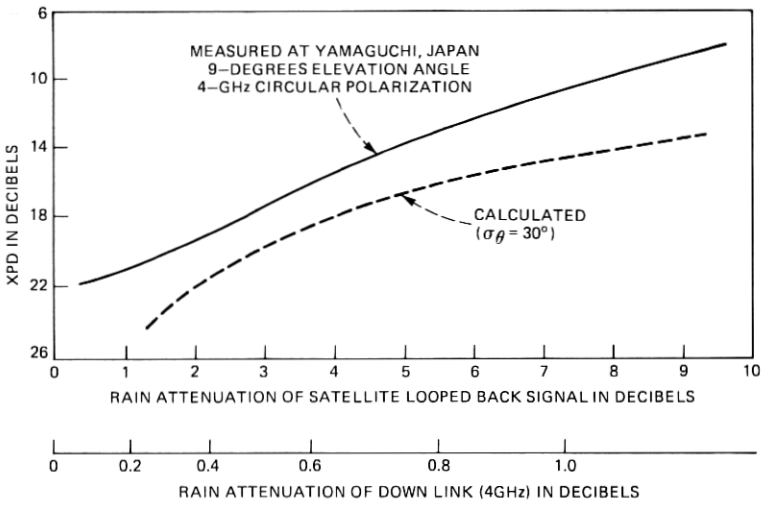

Fig. 3—Comparison between calculated rain-induced cross polarization and measured data from INTELSAT IV. Higher measured values are expected due to ice particle contributions.

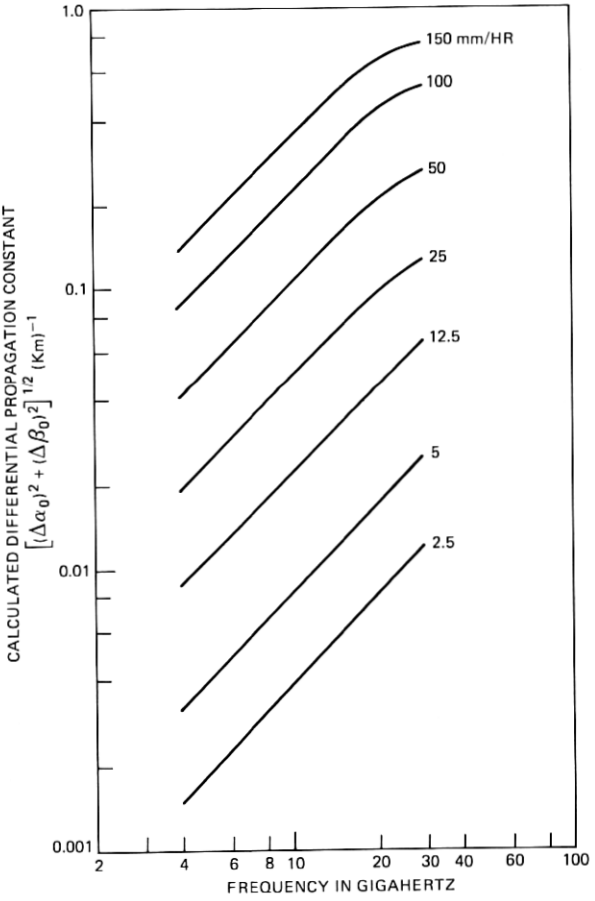

Fig. 4—Calculated differential propagation constant at zero elevation angle vs frequency for various rain rates.

Blacksburg, Virginia with an elevation angle of 33°.[10] The measured cross polarization versus attenuation data at the above two locations have been given respectively as $XPC = -40 + 20.6 \log A$ and $XPC = -41 + 23.2 \log A$, where both XPC and A are in decibel units. Using the procedure described in Section IV, the solid and dotted curves in Fig. 7 are predictions for New Jersey from the Texas and Virginia measurements. The predictions are seen to be in good agreement with the data points[7] for an elevation angle of 27° measured at New Jersey. Extrapolations from Canadian CTS data[11] at an elevation angle of 24.5°, which are not shown here, yield slightly higher cross polarization for a given attenuation. One notes that the Canadian data, which are

confined to attenuation values of less than 10 dB, probably have a higher content of ice particles.

3.4 Linear polarization

The cross polarization of an arbitrary linear polarization is given by eq. (22). For $\sigma_m = 3°$ and 6°, Fig. 8 shows the cross polarization relative to that of a circular polarization which is very close to that of a linear polarization at 45°. This relative cross polarization is independent of frequency. The horizontal and "vertical" polarizations are predicted to have much smaller cross polarization, as is now well known. Recent experiments[4,5] indicate the cross polarization of the preferred horizontal and "vertical" polarization to be 15 to 20 dB below that of circular polarization,[4] i.e., $\sigma_m \approx 3°$ to 6°. Since the measured data appear to be limited by residual system cross polarization ($\lesssim -40$ dB) in clear

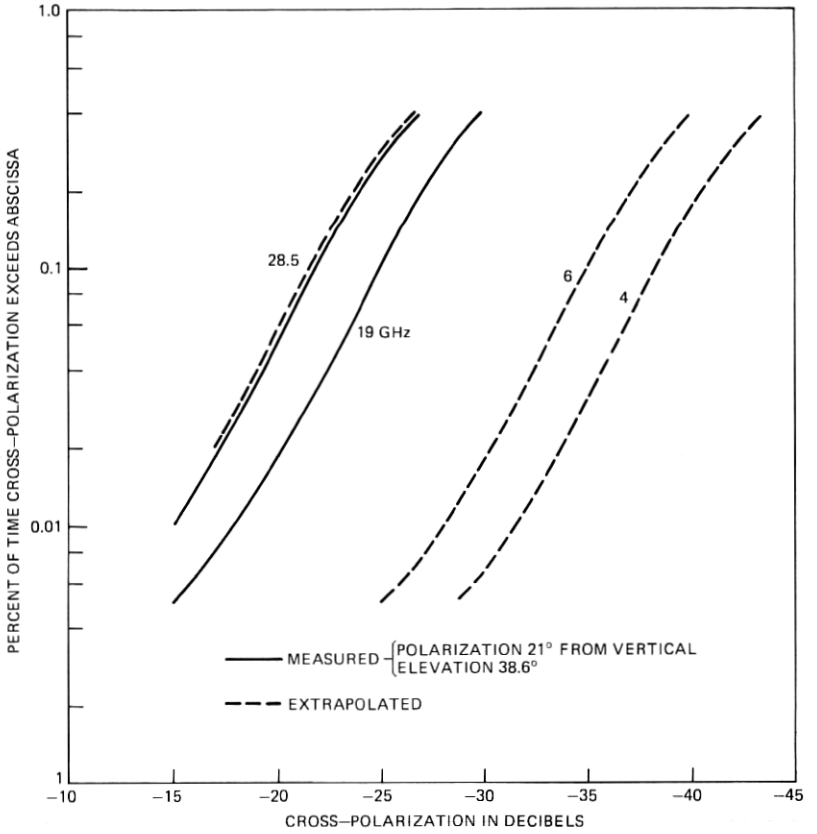

Fig. 5—Measured depolarization statistics and predictions by linear frequency extrapolation from 19-GHz measurements.

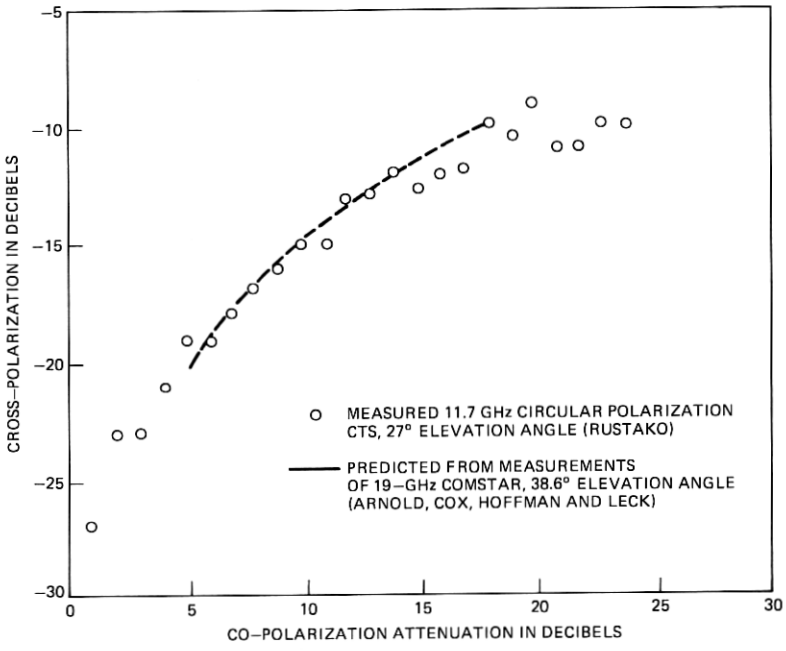

Fig. 6—Comparison between measured 11.7-GHz depolarization at $\theta_{el} = 27°$ and prediction from measured 19-GHz data at $\theta_{el} = 38.6°$.

weather, σ_m is probably 3° or less. The relative cross polarization of an arbitrary linear polarization is not very sensitive to σ_m until the polarization angle becomes smaller than about 10°, where the variation of the relative cross polarization is seen to be within ±1 dB. This observation implies that in spite of the uncertainty about σ_m, using circular polarization data, quantitative prediction can be made of depolarization at most earth stations for an area-coverage linearly polarized satellite. The measured depolarization data[4] of COMSTAR beacon showed that the cross polarization of the linear polarization at 21° from the vertical plane of incidence is lower than that of a circular polarization by 3 dB, which agrees very well with the calculated value in Fig. 8.

3.5 Comparison between two cross-polarization statistics

Circular polarization measurements of 4 GHz at Yamaguchi, Japan using INTELSAT IV at 9° elevation angle recorded rather high cross polarization statistics as shown by the solid curve in Fig. 9, whereas very low cross polarization is shown by the rightmost dotted curve, which is the linear frequency extrapolation to 4 GHz from 19 GHz measurements of Fig. 5 with a linear polarization at 21° from vertical

using the COMSTAR beacon at 38.6° elevation angle. However, if the measured cross-polarization statistics from the COMSTAR beacon are extrapolated to the earth-space path at Japan using the procedure described in Section IV, the leftmost dotted curve is predicted. It is seen that measured results at Japan agree within 2 dB with predictions from COMSTAR measurements. For a given percentage of time, the rain rate at Yamaguchi, Japan is assumed to be greater than that at Holmdel, N.J. by a factor of 1.4, which is inferred from available precipitation data.[8,12,18] The prediction of depolarization statistics is more sensitive to the empirical expression for effective path length, which is a function of elevation angle and rain rate, than the prediction of depolarization versus attenuation. At least part of the discrepancy in Fig. 9 is contributed by the higher residual system cross polarization (−23.5 dB) in INTELSAT measurements.

IV. PROCEDURES OF ESTIMATING CROSS POLARIZATION FOR SATELLITE COMMUNICATION SYSTEMS

For the convenience of system engineers, this section will summarize the procedures for estimating cross-polarization statistics on an earth-space path.

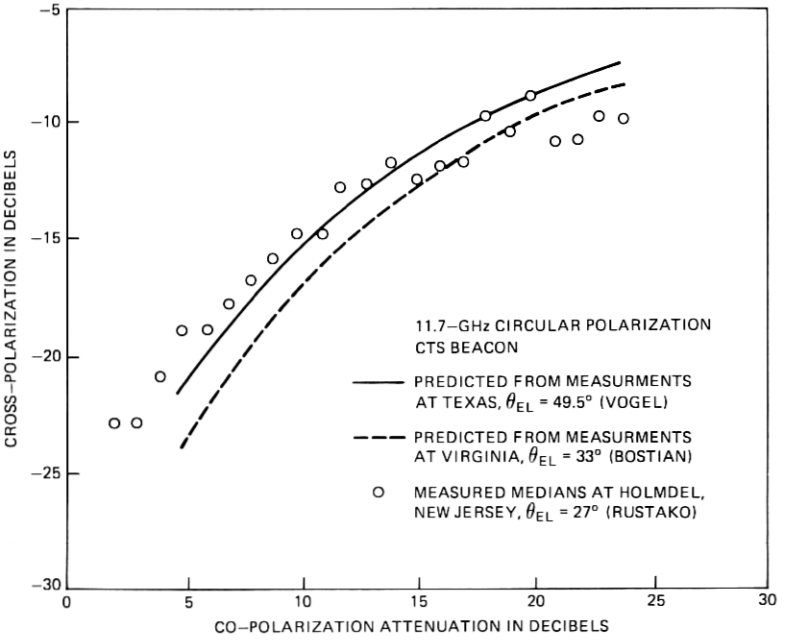

Fig. 7—Comparison between measured 11.7-GHz circularly polarized CTS beacon depolarization at New Jersey and predictions from measured data at Texas and Virginia.

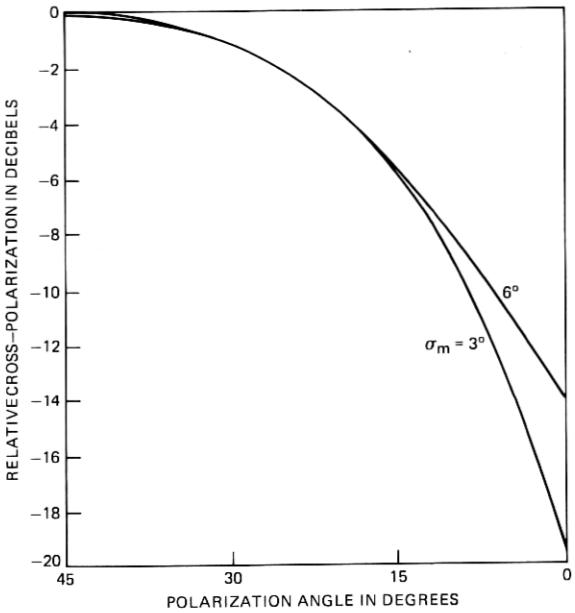

Fig. 8—Calculated cross polarization of an arbitrary linear polarization relative to circular polarization versus polarization angle. Half-differential attenuation (in decibels) should be added and subtracted for quasi-vertical and quasi-horizontal polarizations, respectively.

4.1 Prediction of cross polarization statistics from point rain rate distribution

4.1.1 Calculation from the model

If we are given point rain rate statistics at an earth station antenna of a certain elevation angle, then for any frequency and polarization the expected cross polarization level ($\lesssim -10$ dB) can be calculated as follows. Adding a correction factor of 2 dB for ice-particle depolarization to eq. (24) for circular polarization and to eq. (22) for linear polarization, we have

$$XP_{\text{cir}}(\text{dB}) = 10 \log_{10}\left[\frac{\sinh^2\alpha L + \sin^2\beta L}{\cos^2\beta L + \sinh^2\alpha L}\right] e^{-4\sigma_\theta^2} + 2 \text{ dB} \qquad (28)$$

$$XP_{\text{lin}}(\text{dB}) = XP_{\text{cir}}(\text{dB}) + 10 \log_{10}\frac{1}{2}\left[1 - \cos 4\tau\, e^{-8\sigma_m^2}\right] \pm \frac{\Delta A}{2}, \qquad (29)$$

where τ is the polarization angle from the vertical plane of incidence and $\Delta A/2$ is the differential attenuation factor given by eq (22a). The probable values of the parameters, $\sigma_\theta = 30°$ and $\sigma_m = 3°$, should be expressed in radians. The square bracket in eq. (28) can be approximated by eq. (27), that is,

$$\frac{1}{4}\left[\sqrt{(\Delta\alpha)^2 + (\Delta\beta)^2}L\right]^2,$$

where the differential propagation constant, $\sqrt{(\Delta\alpha)^2 + (\Delta\beta)^2}$, is $\cos^2\theta_{el}$ times those in Fig. 4, and L is the effective path length of eq. (2).

$$L = \frac{1}{(\sin\theta_{el}/h) + (R - 6.2)/2636} \text{ (km)}, \tag{30}$$

where R is the five-minute point rain rate in mm/hr, θ_{el} is the satellite elevation angle, and the rain height h is assumed to be 4 km.

The expected cross polarizations of circularly polarized waves versus rain rate have been computed using eq. (28) for 11 GHz at various elevation angles as shown in Fig. 10. Since the cross polarization amplitude is linearly proportional to frequency for a given earth-space path, the cross polarizations at other frequencies can be approximately

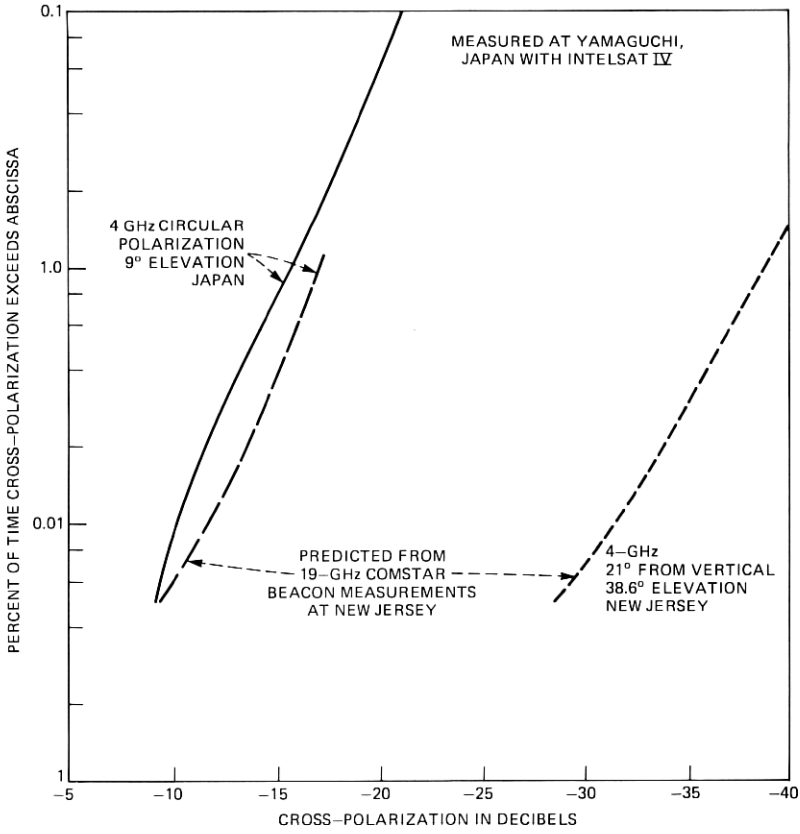

Fig. 9—Comparison between measured 4-GHz circularly polarized INTELSAT IV depolarization statistics at 9° elevation angle and predictions from COMSTAR measurements.

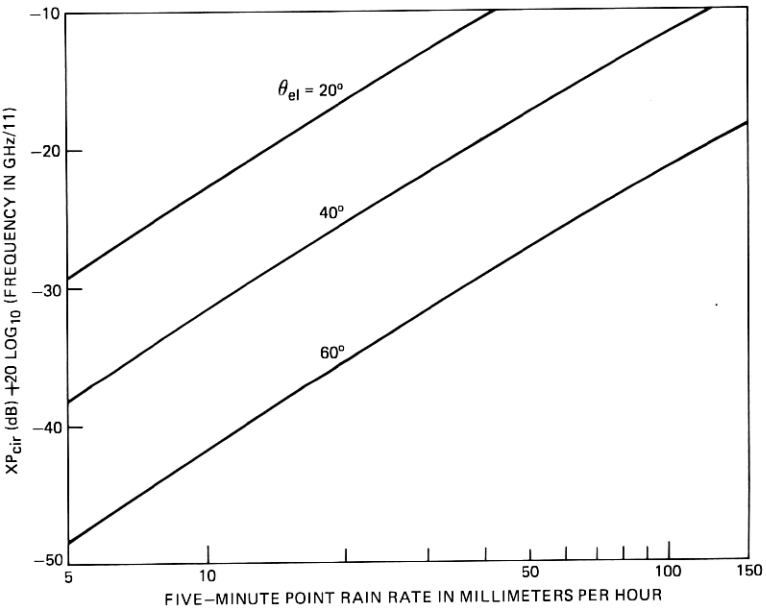

Fig. 10—Expected cross polarization of circularly polarized waves vs rain rate from eq. (28) including 2-dB correction for ice cloud. Ordinates indicate linear frequency dependence of cross-polarization amplitude. Frequency <30 GHz, cross polarization < −10 dB.

determined by adding another factor, $10 \log_{10}(f/11)^2$, which is indicated in the ordinates. To find the cross polarization of linearly polarized waves from eq. (29), the factor $\frac{1}{2}[1 - \cos 4\tau e^{-8\sigma_{in}^2}]$ has been presented in Fig. 8 and the differential attenuation factor $\Delta A/2$ has been computed from eq. (22a) for $\tau = o$ as shown in Fig. 11. For moderate cross polarization ($\lesssim -10$ dB) and small differential attenuation, it is obvious from eq. (20) that the differential attenuation in decibels is approximately proportional to $\cos 2\tau$.

4.1.2 Extrapolation from measured data

The cross polarization statistics of an earth-space path can be predicted from that of another path with different system parameters if point rain rate distributions are available on both paths. The difference between corresponding cross polarizations (in decibels) of paths 1 and 2 for the same percent of time in statistics is given by

$$XP_1(\text{dB}) - XP_2(\text{dB}) = P_1 - P_2 + 20 \log_{10}\left[\frac{(\sqrt{(\Delta\alpha_0)^2 + (\Delta\beta_0)^2})_1 \cos^2\theta_{el_1}}{(\sqrt{(\Delta\alpha_0)^2 + (\Delta\beta_0)^2})_2 \cos^2\theta_{el_2}} \cdot \frac{L_1}{L_2}\right], \quad (31)$$

where the bracket in the logarithmic expression consists of the ratios between differential propagation constants of Fig. 4, $\cos^2\theta_{el}$, and effective path lengths of eq. (30). The polarization factors P are zero for circular polarization and

$$P = 10 \log_{10} \frac{1}{2} [1 - \cos 4\tau \, e^{-8\sigma_m^2}] \pm \frac{\Delta A}{2} \tag{32}$$

for linear polarization is the difference between XP_{lin} and XP_{cir} in eq. (29).

4.2 Prediction of cross polarization statistics from rain attenuation statistics

4.2.1 Calculation from the model

If rain attenuation statistics are already available on an earth-space path, the cross polarization statistics can be obtained from the relation between rain attenuation and cross polarization. This relation is given by calculating the corresponding attenuation and cross polarization for each of a sequence of rain rates. The cross polarization can be calculated from the procedures described in Section 4.1.1, while the attenuation can be calculated from eq. (25) for circular polarization and from eq. (20) for linear polarization. The calculated cross polarization versus attenuation data in Figs. 1, 2, and 3 were obtained by the above method except without the 2-dB correction factor for ice-particle depolarization.

Attenuation versus rain rate for circular polarization from eq. (25) has been presented in Fig. 12 for various elevation angles. Combining

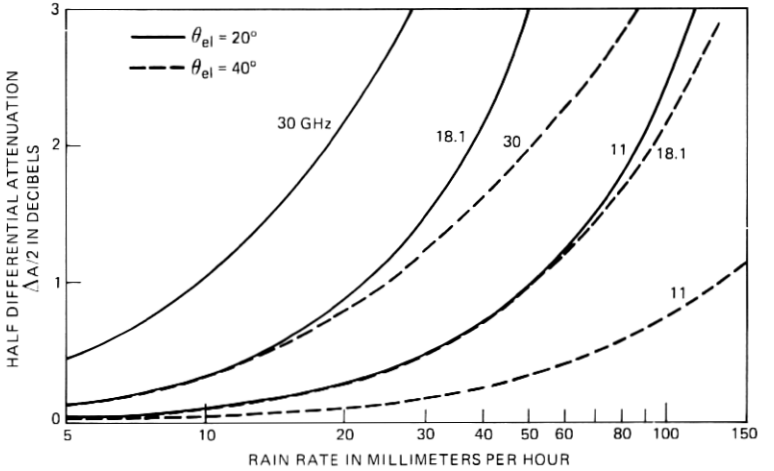

Fig. 11—Differential attenuation between "vertical" and horizontal polarizations ($\tau = 0$) for various frequencies and elevation angles.

Figs. 10 and 12 for each of the corresponding rain rates will yield the cross-polarization-versus-attenuation curve for circular polarization such as those for 11 GHz shown in Fig. 13. The measured 11.7-GHz CTS depolarization versus attenuation data at various elevation angles[7, 9, 10] are also plotted in Fig. 13 for comparison. The relation between rain attenuation and cross polarization for linear polarization can be approximately determined by the following simple additional

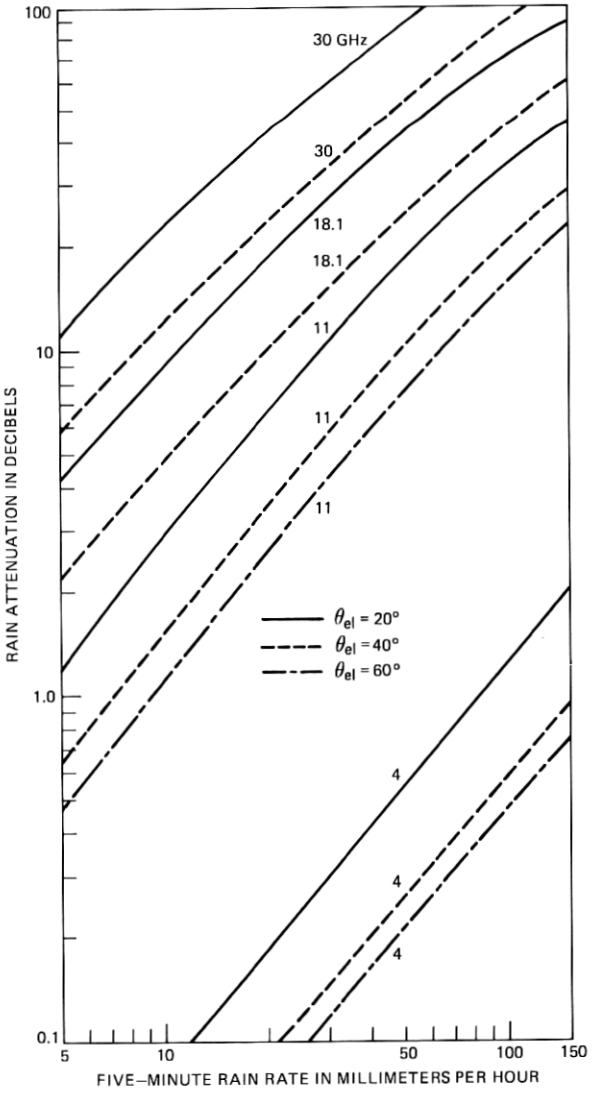

Fig. 12—Rain attenuation vs rain rate for various frequencies and elevation angles.

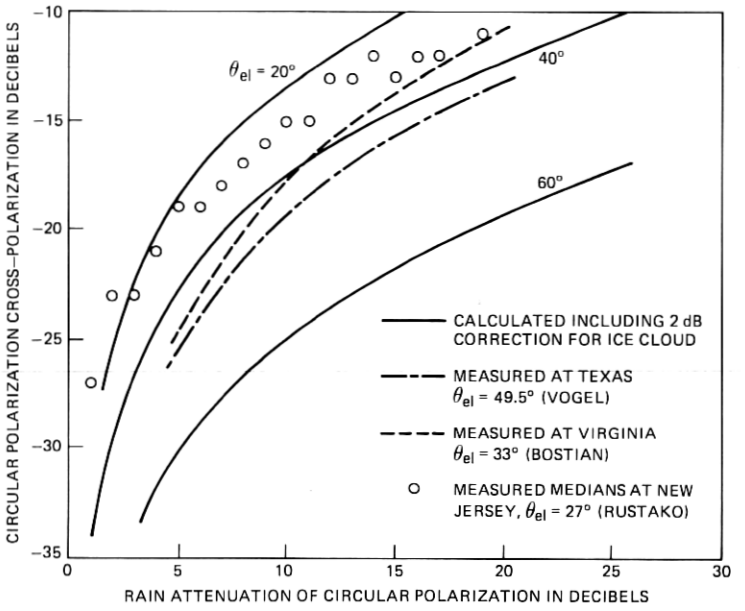

Fig. 13—Comparison between calculated 11-GHz cross polarization vs rain attenuation and measured 11.7 GHz CTS beacon data at various elevation angles.

steps: Fig. 10 will be modified by eq. (20) which is the combination of Figs. 8 and 11, while Fig. 12 will be increased or decreased by the half differential attenuation in Fig. 11.

4.2.2 Extrapolation from measured data

A considerable amount of experimental data on cross polarization versus attenuation are now available. The procedure of extrapolating this relation from one earth-space path to another with different system parameters can be summarized as follows. First, the corresponding attenuations of two cases will be calculated for each of a sequence of rain rates using eq. (25) or (20). Next, the corresponding cross polarization amplitude of the unknown case will be obtained from that of the known case using eq. (31) for the same rain rate.

V. CONCLUSIONS

A two-tier Gaussian model for rain together with the gross features of ice particles have provided a consistent theoretical framework to organize the available experimental data of microwave depolarization of an earth-space path. The differential attenuation and differential phase shift have been approximated by $\cos^2\theta_{el}$ times those for the terrestrial case. An empirical formula for effective path length such as eq. (2) is needed to predict depolarization statistics from point rain-

rate distribution data; however, the effects of frequency and polarization are essentially independent of the uncertainty of empirical path length as well as details of the ice clouds. Both measured depolarization statistics and cross-polarization-versus-attenuation data with different sets of frequency, polarization, and elevation angle have been shown to be predictable from each other using the proposed model.

A linear relation has been found between cross-polarization amplitude and frequency throughout the centimeter wavelengths for a given earth-space path. The dependence of depolarization on orientation of an arbitrary linear polarization is relatively insensitive to the mean canting angle except within about 10° of the vertical or horizontal polarization, whose cross polarizations are about 20 dB below those of circularly polarized waves. A recipe of estimating cross polarization for system engineering together with the probable values of model parameters and typical numerical data have been given in Section IV.

This simple model for prediction of cross polarization has been confirmed by measured medians of long term ($\geq$ 1 year) data. It is *not* to be used for prediction of cross polarization from rain rate or attenuation at any particular instant of time. The short-term relationship between the cross polarization and the attenuation or point rain rate is erratic and difficult to predict. Since the rain-rate distribution strongly depends upon the rain-gauge integration time, caution should be exercised in the application of a rain-rate distribution with integration time other than five minutes. Lin has given an empirical relation among rain rate distributions with integration time from 5 minutes up to 60 minutes.[19]

VI. ACKNOWLEDGMENT

The author is indebted to M. K. Abdelazees, J. W. Carlin, and B. G. Haskell for stimulating discussions and to R. W. England for assistance with the computation.

Note added in proof: Since the rain attenuation (in decibels) is approximately proportional to the square of frequency from 10 to 30 GHz (see Fig. 2 of Ref. 20), the linear frequency dependence of cross-polarization amplitude for a given amount of rain also implies that the rain-induced cross-polarization amplitude in this limited frequency range is inversely proportional to frequency for a given rain attenuation.

REFERENCES

1. T. S. Chu, "Rain-Induced Cross-Polarization at Centimeter and Millimeter Wavelengths," B.S.T.J., *53*, No. 8 (October 1974), pp. 1557–1578.
2. J. A. Morrison and T. S. Chu, "Perturbation Calculations of Rain-Induced Differential Attenuation and Differential Phase Shift at Microwave Frequencies,"

B.S.T.J., *52*, No. 10 (December 1973), pp. 1907–1913.
3. T. Oguchi, "Scattering Properties of Pruppacher-and-Pitter Form Raindrops and Cross Polarizations Due to Rain: Calculations at 11, 13 19.3 and 34.8 GHz," Radio Science, *12* (January–February 1977), pp. 41–51.
4. H. W. Arnold, D. C. Cox, H. H. Hoffman, and R. P. Leck, "Characteristics of Rain and Ice Depolarization for a 19 and 28 GHz Propagation Path From a COMSTAR Satellite," IEEE Transactions, *AP-28* (January 1980), pp. 22–28.
5. H. W. Arnold and D. C. Cox, "Dependence of Depolarization on Incident Polarization for 19 GHz Satellite Signals," B.S.T.J., *57*, No. 9 (November 1978), pp. 3267–3276.
6. H. W. Arnold and D. C. Cox, "Depolarization of 19 and 28 GHz Earth-Space Signals by Ice Particles," Radio Science, *13* (May–June 1978), pp. 511–517.
7. A. J. Rustako, "Measurement of Rain Attenuation and Depolarization of the CTS Beacon Signals at Holmdel, New Jersey," presented at 1979 USNC/URSI Spring Meeting, Seattle, Washington. Preliminary results appear in A. J. Rustako, "An Earth-Space Path Propagation Measurement at Crawford Hill Using the 12-GHz CTS Satellite Beacon," B.S.T.J., *57*, No. 5 (May–June 1978), pp. 1431–1448.
8. H. Kurihara et al, "Degradation of Cross Polarization Discrimination due to Rain on Earth Space Path at Low Elevation Angle," The Transactions of the IECE of Japan, *E61* (October 1978), pp. 848–849. Early results appear in M. Yamada et al, "Rain Depolarization Measurement Using INTETSTAT-IV Sattelite in 4 GHz Band at a Low Elevation Angle," Ann. Telecommunication, *32* (November–December 1977), pp. 524–529.
9. W. J. Vogel, "Some Measrements of CTS 11.7 GHz Cross Polarization Comparing a Fixed and an Adjustable Polarization Receiver," presented at 1979 USNC/URSI Spring Meeting, Seattle, Washington. Early results appear in W. J. Vogel and A. W. Straiton, "CTS Attenuation and Cross-Polarization Measurements at 11.7 GHz," University of Texas report prepared for NASA, April 1977, N78-26349.
10. C. W. Bostian et al, "Summary of 1978 Attenuation and Depolarization Measurements Made with the CTS (11.7 GHz) and COMSTAR (19.04 and 28.56 GHz) Beacons," presented at 1979 USNC/URSI Spring Meeting, Seattle, Washington.
11. J. J. Schlesak, J. I. Strickland, and W. L. Nowland, "Depolarization Measurements at Various Locations Across Canada Using the 11.7 GHz CTS Beacon," presented at 1979 USNC/URSI Spring Meeting, Seattle, Washington. Early results appear in "Measurements of Depolarization and Attenuation at 11.7 GHz by Using the Communications Technology Satellite," Elec. Lett., *13* (November 24, 1977), pp. 750–751.
12. S. H. Lin, "Empirical Rain Attenuation Model for Earth-Satellite Path," IEEE Trans., *COM-27* (May 1979), pp. 812–817.
13. C. Brussaard, "A Meterological Model for Rain-Induced Cross Polarization," IEEE Trans., *AP-24* (January 1976), pp. 5–11.
14. W. L. Nowland, R. L. Olsen, and I. P. Shkarofsky, "Theoretical Relationship Between Rain Depolarization and Attenuation," Elect. Lett. *13* (October 27, 1977), pp. 676–678.
15. V. H. Rumsey et al, "Techniques for Handling Elliptically Polarized Waves with Special Reference to Antennas," Proc. IRE, *38* (May 1951), pp 533–552.
16. D. C. Cox, H. W. Arnold, and H. H. Hoffman, "Differential Attenuation and Depolarization Measurements from a 19 GHz COMSTAR Satellite Beacon Propagation Experiment," presented at USRI Commission F Open Symposium on Propagation in Non-Ionized Media, LaBoule, France, April 29–May 6, 1977.
17. M. J. Saunders, "Cross Polarization at 18 and 30 GHz Due to Rain," IEEE Trans. *AP-19* (March 1971), pp. 273–277.
18. "Local Climatological Data," National Weather Service Office, Newark, New Jersey.
19. S. H. Lin, "Dependence of Rain-Rate Distribution on Rain-Gauge Integration Time," B.S.T.J., *55*, No. 1 (January 1976), pp. 135–141.
20. D. C. Hogg and T. S. Chu, "The Role of Rain in Satellite Communications," Proc. IEEE, *63* (September 1975), pp. 1308–1331.